Talanta 81 (2010) 1446–1453

Contents lists available at ScienceDirect

Talanta

journal homepage: www.elsevier.com/locate/talanta

Computer-assisted design and synthesis of molecularly imprinted polymers for selective extraction of acetazolamide from human plasma prior to its voltammetric determination

Mehdi Khodadadian[a,*], Farhad Ahmadi[b]

[a] Department of Chemistry, Faculty of Science, Razi University, Kermanshah, Iran
[b] Department of Medicinal Chemistry, Faculty of Pharmacy, Kermanshah University of Medical Sciences, Kermanshah, Iran

ARTICLE INFO

Article history:
Received 30 November 2009
Received in revised form 9 February 2010
Accepted 17 February 2010
Available online 25 February 2010

Keywords:
Molecularly imprinted polymer (MIP)
Density functional theory (DFT)
Acetazolamide
Solid-phase extraction (SPE)
Differential pulse voltammetry (DPV)

ABSTRACT

Molecularly imprinted polymers (MIPs) were computationally designed and synthesized for the selective extraction of a carbonic anhydrase inhibitor, i.e. acetazolamide (ACZ), from human plasma. Density functional theory (DFT) calculations were performed to study the intermolecular interactions in the pre-polymerization mixture and to find a suitable functional monomer in MIP preparation. The interaction energies were corrected for the basis set superposition error (BSSE) using the counterpoise (CP) correction. The polymerization solvent was simulated by means of polarizable continuum model (PCM). It was found that acrylamide (AAM) is the best candidate to prepare MIPs. To confirm the results of theoretical calculations, three MIPs were synthesized with different functional monomers and evaluated using Langmuir–Freundlich (LF) isotherm. The results indicated that the most homogeneous MIP with the highest number of binding sites is the MIP prepared by AAM. This polymer was then used as a selective adsorbent to develop a molecularly imprinted solid-phase extraction procedure followed by differential pulse voltammetry (MISPE-DPV) for clean-up and determination of ACZ in human plasma.

1. Introduction

Acetazolamide, *N*-(5-sulfamoyl-1,3,4-thiadiazol-2-yl) acetamide (Scheme 1), is a carbonic anhydrase inhibitor (CAI) used clinically in the management of glaucoma [1]. It is also used, either alone or in association with other antiepileptics, for the treatment of various forms of epilepsy, and is the most frequently used drug for the prophylaxis of high-altitude disorders [2]. The pharmacokinetics of ACZ is well documented in healthy subjects. Absorption is fast, reaching peak plasma concentrations approximately 1–3 h after oral administration. About 80% of the drug is excreted by tubular secretion of the anionic species, and 70–90% of the administered dose is recovered unchanged within 24 h [3].

The determination of ACZ in biological fluids is usually carried out by chromatographic techniques [4–10]. Compared to chromatography, voltammetric techniques have several advantages such as their low cost, sensitivity and short analysis time. However, one of the drawbacks of conventional voltammetric techniques is their low selectivity for target molecules in more complex matrices such as biological samples. To overcome this problem, a clean-up procedure such as liquid–liquid extraction (LLE) or solid-phase extraction (SPE) should be applied to reduce matrix complexity prior to quantitative analysis. In the past, LLE has played a major role in sample clean-up and concentration of the sample components to be measured. However, recovery of sample components by liquid extraction is seldom complete. Liquid extraction tends to be slow and labor-intensive. Additionally, more stringent environmental concerns are making the use and disposal of large amounts of organic solvents more difficult. On the other hand, the popularity and use of SPE are growing at a fast rate. SPE is easily automated, faster, and in general more efficient than LLE. The particles used in SPE are non-polluting and the amount of liquid solvents is tremendously lower than in LLE. Beside these advantages, however, the selectivity of commercial SPE sorbents is low and this makes a problem when a selective extraction from a complex matrix has to be performed.

To enhance the molecular selectivity in SPE, molecularly imprinted polymers (MIPs) [11] have been developed. MIPs are cross-linked macromolecules bearing "tailor-made" binding sites for target molecules. They are prepared by the complexation, in solution, of a target compound (template) with functional monomers, through either covalent or non-covalent bonds, followed by polymerization with an excess of cross-linker to form a highly cross-linked polymer network. Upon removal of the template molecule from the polymer network, specific recognition sites that are complementary to the template in terms of their

* Corresponding author. Tel.: +98 831 4249651; fax: +98 831 4274559.
E-mail address: mehdi.khodadadian@gmail.com (M. Khodadadian).

0039-9140/$ – see front matter © 2010 Elsevier B.V. All rights reserved.
doi:10.1016/j.talanta.2010.02.049

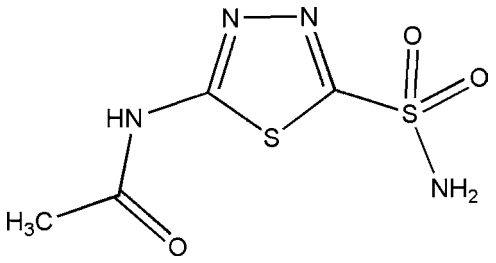

Scheme 1. Chemical structure of acetazolamide (ACZ).

size, shape, and functionality are exposed [12,13]. As a result of their chemical and physical robustness, in combination with the polymer's selectivity, MIPs have proven to be good adsorbents for molecularly imprinted solid-phase extraction (MISPE) applications [14,15]. Nevertheless, general molecular imprinting protocols are tedious and time-consuming because they are based on trial and error method to find the best conditions for imprinting process.

Recently the combinatorial and computational methods have been considered as alternative approaches for the rational design of MIPs [16–18]. The characterization of molecular complexes formed between templates and monomers, with the aim of achieving a clearer picture of the interactions that are the basis of MIP technology, has been the goal of numerous theoretical studies [19]. Over the past few years, a number of studies have been reported describing the application of *ab initio* and DFT computational methods to the rational design of molecularly imprinted polymers [17,20]. The name *ab initio* is given to computations that are derived directly from theoretical principles with no inclusion of experimental data (ab initio is from the Latin: "from first principles"). The *ab initio* method solves the Schrödinger equation for a molecule and gives us the molecule's energy and wavefunction. DFT calculations are, like *ab initio* calculations, based on the Schrödinger equation. However, unlike the *ab initio* method, DFT does not calculate a wavefunction, but rather derives the electron distribution (electron density function) directly. DFT, which has become very popular in recent years, enables novel molecules of theoretical interest to be accurately studied at a lower computational cost as compared to *ab initio* methods [21].

In this work, a DFT-based computational approach was used to the rational design of MIPs for ACZ as template molecule. The MIPs were then synthesized as selective adsorbents to develop a molecularly imprinted solid-phase extraction procedure for efficient clean-up of plasma samples containing ACZ prior to quantitative analysis by differential pulse voltammetry (MISPE-DPV).

2. Experimental

2.1. Materials

Acetazolamide powder (≥99%) was purchased from Sigma (Madrid, Spain). A standard solution of 100 μg mL^{-1} was prepared by dissolving an appropriate amount of ACZ in methanol. This solution was stored at dark and 4 °C. Other diluted solutions were prepared by dilution from the standard solution. Methazolamide and 4-vinylpyridine (4-VP) were purchased from Sigma (Madrid, Spain). Acrylonitrile (ACN), acrylamide (AAM), ethylene glycol dimethacrylate (EGDMA), 2,2′-azobis(isobutyronitrile) (AIBN), trifluoroacetic acid (TFA) and HPLC grade solvents such as methanol (MeOH) and acetonitrile (MeCN) were purchased from Merck (Darmstadt, Germany). ACN, 4-VP and EGDMA were distilled under reduced pressure to remove their stabilizer before use. Human plasma samples were obtained from healthy volunteers and stored at −20 °C until use. All other chemical used were of analytical reagent grade and used without further purification.

2.2. Instrumentation

All voltammograms were recorded using a Metrohm multifunction instrument model 797 VA Computrace. Measurements were carried out with a hanging mercury drop electrode (HMDE) (size: 5), in a three-electrode arrangement. The auxiliary electrode was a wire of platinum with a considerably larger surface area than that of HMDE. An Ag/AgCl electrode was used as reference electrode. Solutions were deoxygenated with high purity nitrogen for 5 min prior to each experiment. All measurements were carried out at room temperature under the nitrogen atmosphere. A Metrohm-780 pH-meter (Switzerland) was used for pH measurements. A Windaus two-channel peristaltic pump model D-38678 was used to pump solvents during MISPE experiments. High performance liquid chromatography (HPLC) was performed on a KNAUER liquid chromatograph system employing EZ-Chrome Elite software. The variable wavelength UV–vis detector was operated at 254 nm for ACZ determination. A 20 μl injection loop and a reversed phase C18 column (250 mm × 4.0 mm i.d., Eurospher 100-5) were used. The mobile phase was 95/3/2 (v/v/v) mixture of 0.4 mol L^{-1} sodium acetate buffer/acetonitrile/methanol adjusted to pH 5.1 at a flow rate of 2 mL min^{-1}.

2.3. General procedure for recording voltammograms

The general procedure for obtaining voltammetric curves was as follows: 10.0 mL of supporting electrolyte (0.1 mol L^{-1} HCl) was transferred into the voltammetric cell and deaerated with high purity nitrogen (99.999%) for 5 min. The voltammetric curve was recorded as background voltammogram over the potential range from −0.2 to −0.8 V using the DPV mode on a HMDE. The required aliquot of the standard solution of ACZ was added by means of a micropipette and its voltammogram was recorded with a new mercury drop as before. The pulse amplitude of 50 mV, pulse width of 40 ms and a scan rate of 40 mV s^{-1} were used for differential pulse voltammetry. All of the electrochemical experiments were carried out at ambient laboratory temperature (25 °C). Between experiments, the cell was treated with concentrated nitric acid and then washed with water.

2.4. Synthesis of polymers

General procedure to prepare imprinted polymers was as follows: the template molecule (0.4 mmol) was mixed with the selected functional monomer (1.6 mmol) in a 10.0 mL screw-capped glass vial followed by the addition of 3.0 mL of acetone as polymerization solvent. The cross-linker EGDMA (6 mmol) and the initiator AIBN (0.12 mmol) were then added to the above solution. To remove dissolved oxygen, the solution was purged with high purity nitrogen (99.999%) for 5 min. Finally, the test tube was sealed under the nitrogen atmosphere and was then placed in a water batch at 50 °C for 12 h. The resultant polymer monolith was crushed, ground mechanically, and sieved. The particle size fraction of 32–63 μm was collected. The template molecule was extracted from the polymers with 90/10 (v/v) MeOH/acetic acid mixture in a Soxhlet extraction system during 24 h. The reference non-imprinted polymers (NIPs) were prepared using the same procedure in the absence of template molecule.

2.5. Binding experiments

Polymer particles (25 mg) were added to 1.0 mL of polymerization solvent, i.e. acetone, containing different concentrations of ACZ and incubated for 12 h at room temperature. After the binding process was completed, the mixture was centrifuged and the concentration of free analyte was determined by DPV. The amount

of ACZ bound to the polymer (B) was calculated by subtracting the amount of free drug (F) from its initial value.

2.6. Molecularly imprinted solid-phase extraction (MISPE)

A 30 mg amount of each dry polymer was packed into empty 3 mL SPE-cartridges between two polyethylene frits. Prior to each extraction, cartridges were conditioned with 2.0 mL of phosphate buffer (1.0×10^{-3} mol L^{-1}, pH 4.0). A 1.0 mL volume of human plasma, spiked with a known concentration of ACZ, was diluted to 2.0 mL with phosphate buffer (pH 4.0) and then percolated through the MIP or NIP cartridge. The cartridge was washed with 1.0 mL of 98/2 (v/v) phosphate buffer (pH 4.0)/MeOH. The drug was eluted from the cartridge by using 2× 0.5 mL of 95/5 (v/v) acetone/TFA. This fraction was then collected and concentrated up to dryness under a nitrogen stream. The sample was then reconstituted with 200 μl of methanol and diluted to 10 mL with supporting electrolyte (0.1 mol L^{-1} HCl), and transferred to the voltammetric cell. The voltammogram was recorded as described in Section 2.3.

2.7. Computational approach

All calculations have been carried out using Gaussian 03 [22] program. The computational method developed was based on density functional theory to locate the most stable template–monomer complexes and the calculation of their electronic stabilization energy relative to isolated fragments, ΔE, through Eq. (1):

$$\Delta E = E(\text{template–monomer complex}) - E(\text{template}) - \sum E(\text{monomer}) \quad (1)$$

A well-known problem in the theory of intermolecular interactions is the occurrence of the so-called basis set superposition error (BSSE) [23]. As two molecules approach each other, the energy of the system falls not only because of the favorable intermolecular interactions but also because the basis functions on each molecule provide a better description of the electronic structure around the other molecule. Despite the well-known existence of BSSE and the means to correct it, only few reports of computationally assisted design of MIPs refer the correction of this error [18,24]. An approximate way of assessing BSSE is the counterpoise (CP) correction [25], which is widely used for the accurate computation of molecular interaction energies by *ab initio* and DFT methods [26,27]. In this method the BSSE is estimated as the difference between monomer energies with the regular basis and the energies calculated with the full set of basis functions for the whole complex. Consider two molecules A and B, each having regular nuclear-centered basis sets denoted with subscripts a and b, and the complex AB having the combined basis set ab. The geometries of the two isolated molecules and of the complex are first optimized or otherwise assigned. The geometries of the A and B molecules in the complex will usually be slightly different than for the isolated species, and the complex geometry will be denoted with an *. The dimer energy minus the monomer energies is the directly calculated complexation energy.

$$\Delta E_{\text{complexation}} = E(\text{AB})^*_{\text{ab}} - E(\text{A})_{\text{a}} - E(\text{B})_{\text{b}} \quad (2)$$

To estimate how much of this complexation energy is due to BSSE, four additional energy calculations are needed. Using the a basis set for A, and the b basis set for B, the energies of each of the two fragments are calculated with the geometry they have in the complex. Two additional energy calculations of the fragments at the complex geometry are then carried out with the full ab basis set. This means that the energy of A is calculated in the presence of both the normal a basis functions and with the b basis functions of fragment B located at the corresponding nuclear positions, but without the B nuclei present, and vice versa. Such basis functions located at fixed points in space are often referred to as ghost orbitals. The fragment energy for A will be lowered due to these ghost functions, since the a basis becomes more complete. The CP correction is defined in Eq. (3) [27].

$$\Delta E_{\text{CP}} = E(\text{A})^*_{\text{ab}} + E(\text{B})^*_{\text{ab}} - E(\text{A})^*_{\text{a}} - E(\text{B})^*_{\text{b}} \quad (3)$$

The counterpoise-corrected complexation energy is then given as $\Delta E_{\text{complexation}} - \Delta E_{\text{CP}}$.

Because polymerization is occurred in solution, we must take into account the effect of solvent, or solvation, in energy calculations because it leads to changes in energy and stability of the template–monomer complexes. Methods for evaluating the solvent effect may broadly be divided into two types: those describing the individual solvent molecules and those that treat the solvent as a continuous medium [28–30]. Continuum models [31], which are more popular, consider the solvent as a uniform polarizable medium with a dielectric constant of ε, while the solute is placed in a suitably shaped cavity in the medium [32]. In this section, the polarizable continuum model (PCM), developed by Tomasi and coworkers [33–35], was used to study the effect of solvent in energy calculations.

In this study, electronic energies were calculated through DFT method at B3LYP/6-31G(d) level. The optimized geometries were further optimized by application of the CP method at B3LYP/6-31G(d) level for the correction of BSSE error. In order to introduce the effect of solvent in energy calculations, the polarizable continuum model (PCM) was used.

3. Results and discussion

3.1. Theoretical study of template–monomer interactions

The selection of suitable functional monomers for imprinting process may be aided by molecular modeling and computational methods [36]. In a typical computational approach, a virtual library of functional monomers is created and screened for all possible interactions between monomers and the template molecule. Monomers with the highest binding scores are subsequently selected to produce full scale MIPs with hopefully superior recognition properties. In this work, eight functional monomers, i.e. acrylamide (AAM), 4-vinylpyridine (4-VP), methacrylic acid (MAA), acrylic acid (AA), 2-(trifluoromethyl)-acrylic acid (TFMAA), acrylonitrile (ACN), methyl methacrylate (MMA), and methacrylamide (MAAM) were theoretically selected as possible functional monomers. The conformation of template, functional monomers and template–monomer complexes was optimized to the lowest energy using DFT method at B3LYP/6-31G(d) level. As an example, Fig. 1 shows the optimized geometries of 1:1, 1:2 and 1:3 template–monomer complexes between ACZ and AAM. Table 1 summarizes the calculated interaction energies for all complexes formed between ACZ and functional monomers before and after BSSE correction in the gas-phase. As can be seen, the values of binding energy are influenced by BSSE with a slight variation in stability order. It is also observed that the 1:3 complexes are the most stable structures. In solution, however, the stability and order of binding energy are quite different. Table 2 lists the data for 1:3 complexes. The interaction energies obtained with different implicit solvents correspond in every case to a significant decrease as compared to the gas-phase interaction. This makes sense since solvation of a species involves also intermolecular interactions of the same nature as monomer–template and so the solvent acts as a competitor. From the data listed in Table 2, it is concluded that the combination of AAM and acetone leads to the most stable complexes. To examine the accuracy of the theoretical calculations, several polymers

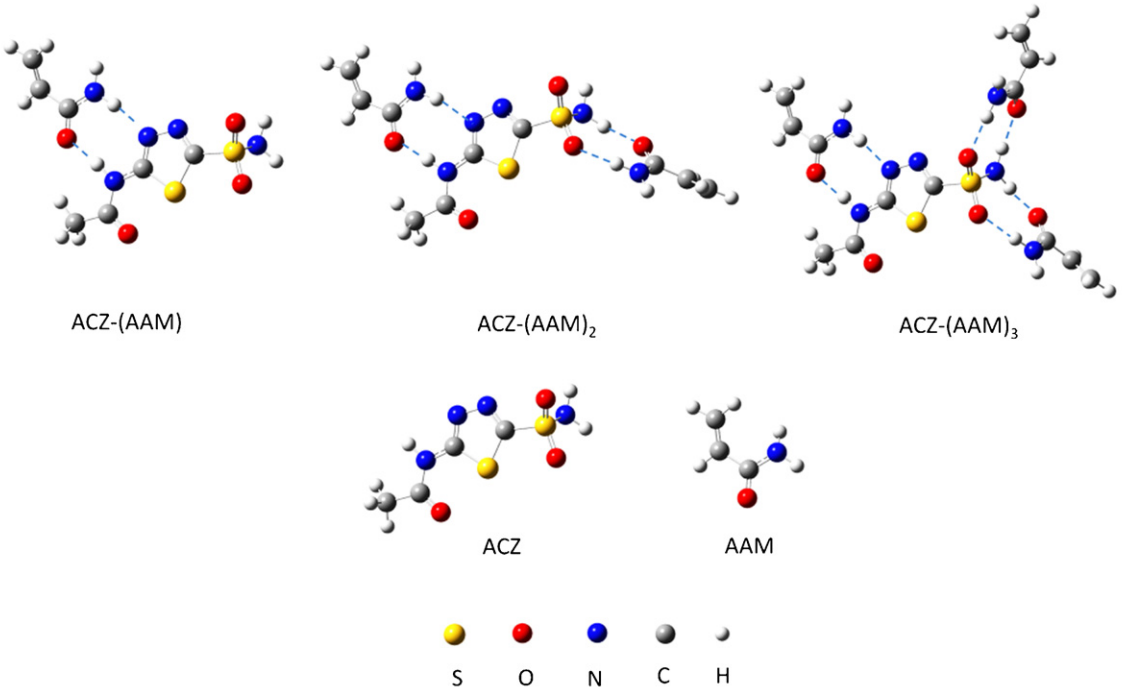

Fig. 1. Computationally derived structures of 1:1, 1:2 and 1:3 complexes of ACZ with AAM using DFT method at B3LYP/6-31G(d) level.

Table 1
Calculated interaction energies (ΔE, kJ mol^{-1}) for 1:1, 1:2 and 1:3 template–monomer complexes with and without BSSE correction in the gas-phase.

Complexes	$\Delta E_{\text{non-corr}}$	ΔE_{corr}
ACZ–(TFMAA)	−87.051	−73.027
ACZ–(AA)	−85.999	−71.041
ACZ–(MAA)	−84.754	−34.406
ACZ–(AAM)	−83.573	−68.496
ACZ–(MAAM)	−82.645	−41.029
ACZ–(4-VP)	−53.591	−40.387
ACZ–(MMA)	−49.068	−34.234
ACZ–(ACN)	−42.130	−29.679
ACZ–(TFMAA)$_2$	−151.722	−124.230
ACZ–(AA)$_2$	−149.645	−121.552
ACZ–(MAA)$_2$	−148.162	−119.652
ACZ–(AAM)$_2$	−146.622	−118.462
ACZ–(MAAM)$_2$	−144.424	−117.001
ACZ–(4-VP)$_2$	−95.618	−75.705
ACZ–(MMA)$_2$	−92.286	−76.589
ACZ–(ACN)$_2$	−88.231	−72.121
ACZ–(TFMAA)$_3$	−210.486	−171.220
ACZ–(AA)$_3$	−208.909	−167.924
ACZ–(MAA)$_3$	−206.403	−165.264
ACZ–(AAM)$_3$	−201.467	−160.656
ACZ–(MAAM)$_3$	−200.104	−158.395
ACZ–(4-VP)$_3$	−130.451	−101.829
ACZ–(MMA)$_3$	−110.518	−78.4202
ACZ–(ACN)$_3$	−105.847	−81.4446

Table 2
Calculated interaction energies (ΔE, kJ mol^{-1}) for1:3 template–monomer complexes in different solvents.

Complexes	Acetone	MeCN	MeOH	DMSO	Water
ACZ–(AAM)$_3$	−91.498	−87.453	−88.232	−84.442	−84.835
ACZ–(MAAM)$_3$	−88.897	−85.199	−86.367	−83.404	−83.197
ACZ–(AA)$_3$	−71.439	−66.611	−67.497	−64.915	−63.623
ACZ–(MAA)$_3$	−69.177	−64.561	−65.801	−63.411	−62.111
ACZ–(4-VP)$_3$	−64.518	−62.285	−63.007	−61.127	−61.261
ACZ–(TFMAA)$_3$	−63.020	−58.455	−50.165	−55.567	−56.229
ACZ–(MMA)$_3$	−34.463	−32.450	−33.501	−32.854	−31.905
ACZ–(ACN)$_3$	−13.665	−11.753	−12.708	−9.3231	−11.690

for ACZ were prepared by bulk polymerization using ACN (MIP1), 4-VP (MIP2) and AAM (MIP3) as functional monomers, EGDMA as cross-linker and acetone as polymerization solvent.

3.2. Adsorption isotherm

In this section, the heterogeneous Langmuir–Freundlich (LF) isotherm was considered for the evaluation of binding characteristics of the synthesized MIPs [37]. The LF isotherm describes a relationship between the concentration of bound (B) and free (F) guest in heterogeneous systems with three different coefficients according to the following equation:

$$B = \frac{N_t a F^m}{1 + a F^m} \quad (4)$$

where N_t is the total number of binding sites, a is related to the median binding affinity constant (K_0) via ($K_0 = a^{1/m}$), and m is the heterogeneity index, which will be equal to 1 for a homogeneous material, or will take values within 0 and 1 if the material is heterogeneous.

The experimental isotherm data (F and B) were successfully fitted to the LF isotherm in order to evaluate the N_t, K_0, and m values (Fig. 2 is shown as an example for MIP3). The resulted fitting coefficients at the desired concentration window are listed in Table 3. As seen, the value of m demonstrates the heterogeneity of all MIPs. However, MIP3 shows the highest degree of binding site homogeneity with the highest heterogeneity index ($m = 0.51$). The comparison of other binding parameters reveals

Table 3
Langmuir–Freundlich isotherm fitting coefficients for MIP1, MIP2 and MIP3.

Polymer	Isotherm parameters				R^2
	N_t (μmol g^{-1})	a (g μmol^{-1})	m	K_0 [a] (g μmol^{-1})	
MIP1	333.4	0.040	0.45	8.0×10^{-4}	0.9997
MIP2	445.2	0.041	0.49	1.4×10^{-3}	0.9994
MIP3	683.3	0.044	0.51	2.2×10^{-3}	0.9997

[a] The mean association constant which was calculated as $K_0 = a^{1/m}$.

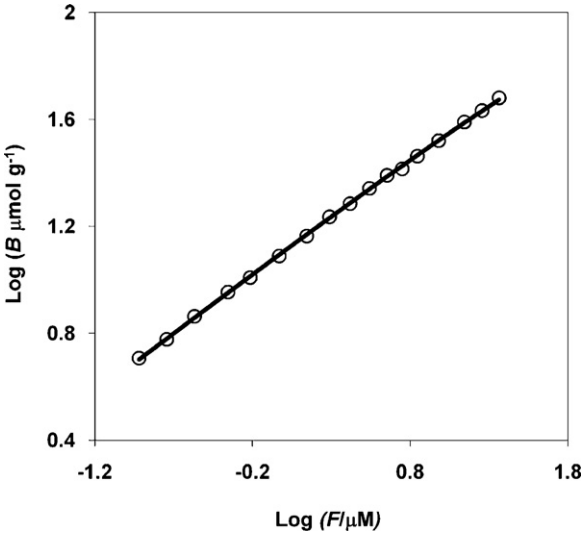

Fig. 2. Experimental isotherm (circle) and LF fit (line) for MIP3.

that MIP3 has the highest concentration of binding sites per gram of polymer (N_t = 683.3 μmol g^{-1}) and median binding affinity ($K_0 = 2.2 \times 10^{-3}$ μmol^{-1}). From Table 3 it is also concluded that the results of LF isotherm are consistent with the theoretical calculations.

From the theoretical molecular modeling studies and binding experiments, the MIP3 which is manufactured by AAM was identified as the favored imprinted material for use in the subsequent MISPE experiments.

3.3. Voltammetric behavior of ACZ

To elucidate the electrode reaction of ACZ, cyclic voltammograms of the drug were recorded at HMDE and at different scan rates. Fig. 3 shows the cyclic voltammograms of the drug (1.0×10^{-5} mol L^{-1}) in 0.1 mol L^{-1} HCl solution. The voltammograms exhibit one well-defined cathodic peak at about −480 mV, with no peak on the reverse scan, suggesting the irreversible nature of the electrode reaction. The effect of potential scan rate, ν, on the peak current of ACZ was evaluated and is shown in the inset of Fig. 3. A linear relationship was observed between log i_p and log ν over the scan range 10–550 mVs^{-1} (r^2 = 0.9993) and corresponds to

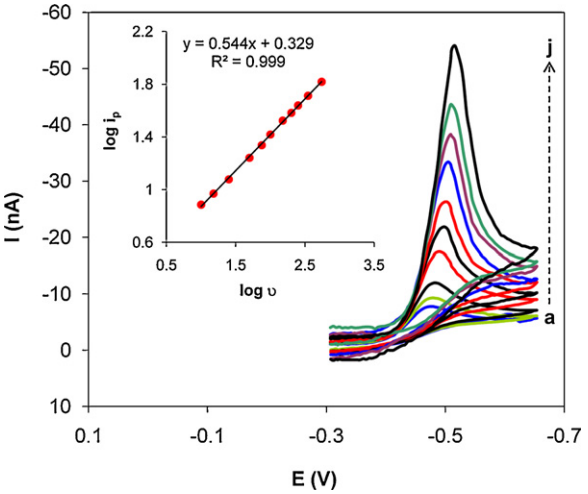

Fig. 3. Cyclic voltammograms of 1.0×10^{-5} mol L^{-1} ACZ in 0.1 mol L^{-1} HCl recorded at different scan rates (a–j: 10–550 mVs^{-1}), and corresponding log i_p vs. log ν plot.

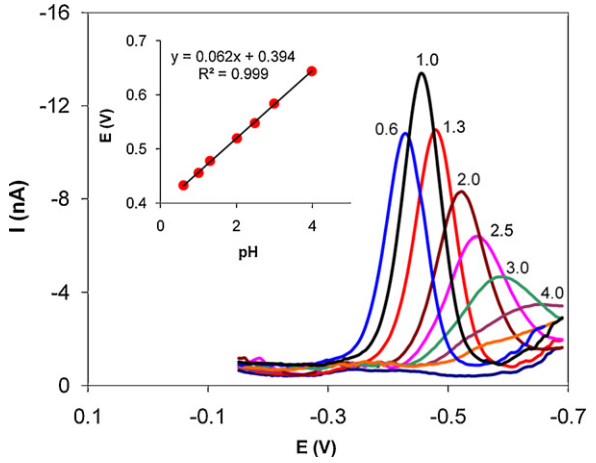

Fig. 4. Effect of pH on the differential pulse voltammograms of 1×10^{-7} mol L^{-1} ACZ. Instrumental parameters were: pulse amplitude 50 mV, pulse with 40 ms, scan rate 40 mV s^{-1}.

the equation log i_p = 0.544 log ν + 0.329 (i_p in nA and ν in Vs^{-1}). The slope of 0.544 is close to the theoretically expected value of 0.50 for a diffusive process [38]. On the other hand, as scan rate increased, the potential shifted to more negative values as expected for an irreversible reduction process [39]. In a study of the peak potentials shift as a function of scan rate, the peak potential (E_p) of the cathodic wave was observed to move cathodically by increasing sweep rates. The plot of $E_p = f(\log \upsilon)$ resulted in a straight line ($r^2 > 0.998$) with a slope of 30.3 mV/decade ($30/\alpha n_a$) [40]. So the αn_a value is 0.97. Since the value of α is normally considered to be 0.5, the number of electrons, n_a, transferred in the rate-determining step should be two (n_a = 2). The presence of azomethine reducible group (–C=N–) in the structure of ACZ is probably responsible for the observed reduction wave.

In order to develop a voltammetric method for determining the drug, we selected the DPV mode, since the peak was sharper and better defined than that obtained by cyclic voltammetry, with lower background current. The DPVs of 1.0×10^{-6} mol L^{-1} ACZ were obtained at different pHs (HCl and phosphate buffers were used for adjusting the test solution pHs) (Fig. 4). The wave was well developed at pH < 4. The potential of the cathodic peak of ACZ was shifted linearly towards more negative potentials by increasing the pH between 0.6 and 4.0. The slope 62 mV/pH confirms the participation of equal number of electrons and protons in the reduction process. As can be seen from Fig. 4, at pH 1.0 the maximum signal is obtained. Thus, 0.1 mol L^{-1} HCl was used as background electrolyte throughout the present study.

The influence of electrochemical parameters known to affect the differential pulse voltammograms, viz. pulse amplitude, pulse width and scan rate were studied. During the study, each variable was changed while the other two were kept constant. The variables of interest were studied over the ranges 25–100 mV for pulse amplitude, 30–100 ms for pulse width and 10–60 mV s^{-1} for scan rate. It was found that the peak height increased by increasing scan rate, however, the peak current decreased as the pulse width increased. To acquire voltammograms of relatively high sensitivity and well-shaped waves with relatively a narrow peak width, values of 50 mV, 40 ms and 40 mV s^{-1} were chosen for pulse amplitude, pulse width and scan rate, respectively.

3.4. Optimization of MISPE procedure

3.4.1. Effect of pH

To have better interaction between MIP and target molecule in aqueous media, the effect of sample pH should be studied. The effect

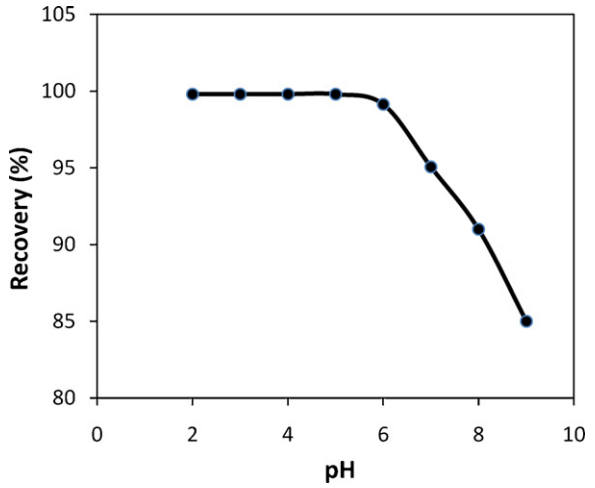

Fig. 5. Effect of pH on the recovery of ACZ from MIP3 cartridge.

of buffer pH on ACZ binding was investigated over the pH range 2.0–9.0 for MIP3 (Fig. 5). Clearly, the binding behavior of ACZ was not greatly affected at pH < 6.0. However, at more alkaline pHs the recovery of the drug was considerably decreased as pH increased. It has been reported that ACZ has two pK_a values [41]. The pK_1 corresponds to the dissociation of carbonamido group (p$K_1 \approx 7.2$) and pK_2 arises from the dissociation of sulfonamido group under alkaline conditions (p$K_2 \approx 9.0$) [42]. At pH < 6.0 ACZ is fully protonated and therefore the selective binding to the MIP is mainly due to hydrogen bonds. At more alkaline solutions ACZ is deprotonated and the hydrogen bonds between the drug and MIP failed, therefore the selective binding interaction reduced. The pH 4.0 was selected for subsequent MISPE experiments.

3.4.2. Selection of washing solvent

Washing MIP is a crucial step in developing a MISPE procedure because the general procedure for reducing problems of non-specific adsorption is the selection of a proper washing solvent prior to elution [43]. Thus, in this section we test several washing solvents to develop an efficient washing step. The results are shown in Fig. 6. As can be seen, when cartridges were washed with 1.0 mL of acetone or MeOH the recovery of the drug decreased considerably. Nevertheless, when 1.0 mL of 98:2 (v/v) phosphate buffer (pH 4.0)/MeOH was used as washing solvent, the recovery of the drug from MIP and NIP was 98.3% and 6.3%, respectively. From Fig. 6 it is also concluded that a 98/2 (v/v) mixture of phosphate buffer (pH 4.0) and MeOH leads to the maximum difference between MIP's and NIP's recovery. Therefore, this mixture was selected as washing solution as it combines a good recovery and a high degree of specific retention on MIP.

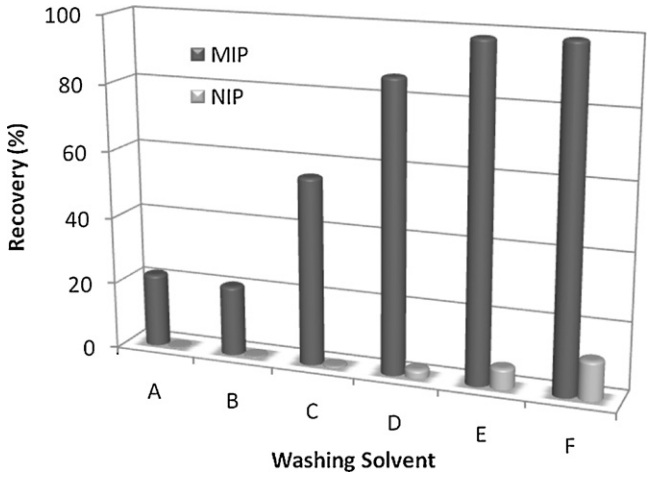

Fig. 6. ACZ recoveries (%) from MIP3 and NIP3 cartridges after washing the cartridges with 1.0 mL of: (A) MeOH, (B) acetone, (C) 50:50, (D) 90:10, (E) 98:2, and (F) 98:1 (v/v) phosphate buffer (pH 4.0)/MeOH. 2× 0.5 mL of 95/5 (v/v) acetone/TFA was used for the elution step.

Table 4
Typical recovery of acetazolamide from MIP3 cartridge using different elution solvents. The volume of solvent in each step was 0.5 mL.

Elution solvent	First (%)	Second (%)	Third (%)	Total (%)
Acetone	68.3	13.9	9.7	91.9
MeOH	67.1	13.0	8.6	88.7
MeCN	42.5	11.8	7.7	62.0
Acetone + 2% TFA	82.6	14.9	1.8	99.3
Acetone + 5% TFA	83.9	15.7	<0.1	99.7

3.4.3. Selection of elution solvent

The specific interactions between MIP and template molecule are non-covalent, e.g. hydrogen bonds, and can be destroyed by the polar solvents, such as MeOH, MeCN, acetone, and binary mixtures of acetone and TFA. The best recoveries were obtained using acetone containing 5% TFA (Table 4). Therefore, 2× 0.5 mL of 95/5 (v/v) acetone/TFA was used as elution solution throughout the present study.

3.5. Validation of the method

The MISPE-DPV method for the determination of ACZ was validated by determining its performance characteristics regarding linearity, repeatability, and precision. To test the DPV response linearity, a series of standard solutions of ACZ in the concentration range 0.20–18.0 μg mL^{-1} were analyzed (at least ten samples covering the whole range were used). The relationship between peak height (y, nA) and concentration (x, μg mL^{-1}) was linear for ACZ according to the equation $y = 41.967x + 0.338$; ($R^2 = 0.9982$) ($n = 15$). As defined by European Pharmacopoeia [44], the LOQ and LOD are the concentrations at which the signal-to-noise ratio is 3 and 10, respectively. The limit of detection (LOD) and the limit of quantification (LOQ) were 0.06 and 0.20 μg mL^{-1}, respectively. The RSD

Table 5
Distribution ratio (K_d) and selectivity coefficient (α) values for imprinted and non-imprinted polymers.

Compound	MIP		NIP	
	K_d	α	K_d	α
Acetazolamide	96.2		16.5	
Methazolamide	29.6	3.25	11.3	1.46
Hydrochlorothiazide	17.6	5.46	14.8	1.11
Zonisamide	28.3	3.39	18.5	0.89
Guaifenesin	12.2	7.88	13.7	1.20
Metronidazole	16.1	5.97	11.5	1.43

Table 6
Tolerable concentration ratios with respect to acetazolamide for some interfering substances using DPV and MISPE-DPV.

Interfering substances	DPV	MISPE-DPV
Starch	250	2300
Urea, citric acid	200	1700
Uric acid	150	1000
Glucose, sucrose, ascorbic acid	100	850
Creatinine, leucine, glycine	75	800
Histidine, arginine	8	400
Glutathione	1	450
Cysteine	0.02	150

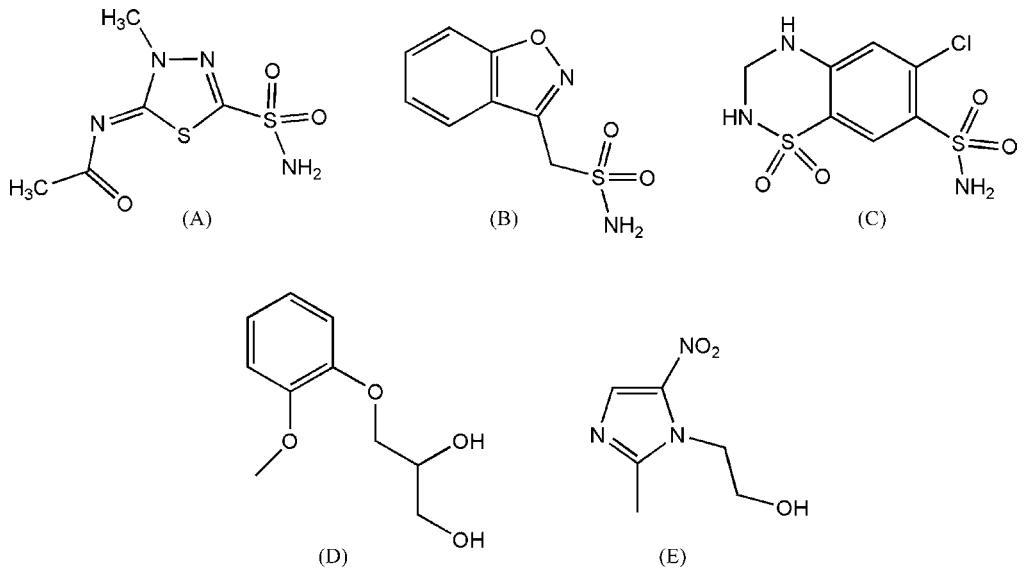

Scheme 2. Chemical structures of: (A) methazolamide, (B) zonisamide, (C) hydrochlorothiazide, (D) guaifenesin, and (E) metronidazole.

Table 7
Results of determination of ACZ in plasma ($n = 5$).

Concentration ($\mu g\,mL^{-1}$)	MISPE-DPV ($\mu g\,mL^{-1}$)	HPLC ($\mu g\,mL^{-1}$)	*t*-Test[a]	*F*-test
0.5	0.466 ± 0.021	0.479 ± 0.026	0.77	1.53
1.0	0.965 ± 0.029	0.935 ± 0.018	1.75	2.59
5.0	4.820 ± 0.191	4.906 ± 0.182	0.65	1.10

[a] Theoretical values of t and F at $P = 0.05$ are 2.31 and 6.39, respectively.

value for intraday assay reproducibility at 0.5 $\mu g\,mL^{-1}$ solution ($n = 5$) was found to be 2.86% indicating good repeatability of the method.

3.6. The selectivity test

In order to evaluate the selectivity of the synthesized MIP, methazolamide, which is an analogue of ACZ, and several drugs with different structures but able to form hydrogen bonds with the MIP were considered in this section (Scheme 2). In several batch experiments, the distribution ratios (K_d) and selectivity coefficients (α) were calculated and are listed in Table 5.

The K_d values were calculated using the equation:

$$K_d = \frac{(C_i - C_f)V}{C_f m}$$

where V, C_i, C_f and m represent the volume of the solution (mL), drug concentration before and after adsorption ($\mu g\,mL^{-1}$) and mass of the polymer, respectively. The selectivity coefficient (α) is defined as:

$$a = \frac{K_d(\text{acetazolamide})}{K_d(\text{foreign compound})}$$

The results from Table 5 clearly suggest that the unique shape of the template molecule plays an important role in its selective binding to the MIP.

3.7. Interference study

Under the selected conditions for determining the drug, the interference of some species commonly present in biological media was examined by analyzing a standard solution of 0.5 $\mu g\,mL^{-1}$ ACZ. The tolerable limit of foreign species was considered with the relative error less than 3%. The results are listed in Table 6. These results clearly show that MIP can be used as a good adsorbent for clean-up of complex samples to improve the selectivity of the DPV method.

3.8. Evaluation of MISPE-DPV for plasma samples

The applicability of the MISPE-DPV method was tested for human plasma samples. In order to validate the methodology and confirm its potential in routine monitoring of ACZ, the same samples were subjected to a previously reported HPLC method [9]. Table 7 compares the results of the analysis of ACZ between the two methods. As can be seen, the methods show similar accuracy and precision at the concentrations tested as revealed by the *t*-test and *F*-test, respectively.

4. Conclusion

The results of the present study show that the computer-assisted design of MIPs based on density functional theory (DFT) can be used as a powerful tool to screen functional monomers for a specified template molecule. The DFT calculations predict that AAM/acetone is the best combination of functional monomer/solvent which leads to the most stable pre-polymerization complexes with ACZ as template. Adsorption isotherm studies also showed that the MIP prepared by AAM is the most homogeneous MIP with the highest number of binding sites. This polymer was then used as a selective adsorbent to develop a molecularly imprinted solid-phase extraction (MISPE) procedure for selective extraction of ACZ from human plasma before differential pulse voltammetry (DPV). The combination of MISPE and differential pulse voltammetry (DPV) considerably enhanced the selectivity of the voltammetric technique. The developed MISPE-DPV method exhibited good analytical performance in terms of selectivity, sensitivity, reproducibility and accuracy for quantification of ACZ in complex biological samples such as human plasma.

References

[1] P. Kaur, R. Smitha, D. Aggarwal, M. Kapil, Int. J. Pharm. 248 (2002) 1.
[2] Martindale, The Complete Drug Reference, 32nd ed., Pharmaceutical Press, London, UK, 1999.
[3] W.A. Ritschel, C. Paulos, A. Arancibia, M.A. Agrawal, K.M. Wetzelsberger, P.W. Lucker, J. Clin. Pharmacol. 38 (1998) 533.
[4] D.M. Chambers, M.H. White, H.B. Kostenbauder, J. Chromatogr. 225 (1981) 231.
[5] D.J. Chapron, L.B. White, J. Pharm. Sci. 73 (1984) 985.
[6] R. Hartley, M. Lucock, M. Becker, I.J. Smith, W.I. Forsythe, J. Chromatogr. 377 (1986) 295.
[7] R. Herraez-Hernandez, P. Campins-Falco, A. Sevillano-Cabeza, J. Chromatogr. 120 (1992) 181.
[8] N. Ichikawa, K. Naora, H. Hirano, K. Iwamoto, J. Pharm. Biomed. Anal. 17 (1998) 1415.
[9] A. Zarghi, A. Shafaati, J. Pharm. Biomed. Anal. 28 (2002) 169.
[10] US Pharmacopoeia, 24th ed., U.S. Pharmacopoeial Convention, Rockville, MD, USA, 2000.
[11] O. Ramström, R.J. Ansell, Chirality 10 (1998) 195.
[12] B. Sellergren, L.I. Andersson, Methods 22 (2000) 92.
[13] K. Ensing, T. de Boer, Trends Anal. Chem. 18 (1999) 138.
[14] L.I. Andersson, J. Chromatogr. B 739 (2000) 163.
[15] D. Stevenson, Trends Anal. Chem. 18 (1999) 154.
[16] Y. Li, X. Li, Y. Li, C. Dong, P. Jin, J. Qi, Biomaterials 30 (2009) 3205.
[17] J. Yao, X. Li, W. Qin, Anal. Chim. Acta 610 (2008) 282.
[18] M. Azenha, P. Kathirvel, P. Nogueira, A. Fernando-Silva, Biosens. Bioelectron. 23 (2008) 1843.
[19] I.A. Nicholls, H.S. Andersson, C. Charlton, H. Henschel, B.C.G. Karlsson, J.G. Karlsson, J. O'Mahony, A.M. Rosengren, K.J. Rosengren, S. Wikman, Biosens. Bioelectron. 25 (2009) 543.
[20] M.B. Gholivand, M. Khodadadian, F. Ahmadi, Anal. Chim. Acta 658 (2010) 225.
[21] D.C. Young, Computational Chemistry: A Practical Guide for Applying Techniques to Real-world Problems, John Wiley & Sons, Inc., New York, 2001.
[22] M.J. Frisch, G.W. Trucks, H.B. Schlegel, G.E. Scuseria, M.A. Robb, J.R. Cheeseman, V.G. Zakrzewski, J.J.A. Montgomery, R.E. Stratmann, J.C. Burant, S. Dapprich, J.M. Millam, A.D. Daniels, K.N. Kudin, M.C. Strain, O. Farkas, J. Tomasi, V. Barone, M. Cossi, R. Cammi, B. Mennucci, C. Pomelli, C. Adamo, S. Clifford, J. Ochterski, G.A. Petersson, P.Y. Ayala, Q. Cui, K. Morokuma, D.K. Malick, A.D. Rabuck, K. Raghavachari, J.B. Foresman, J. Cioslowski, J.V. Ortiz, B.B. Stefanov, G. Liu, A. Liashenko, P. Piskorz, I. Komaromi, R. Gomperts, R.L. Martin, D.J. Fox, T. Keith, M.A. Al-Laham, C.Y. Peng, A. Nanayakkara, C. Gonzalez, M. Challacombe, P.M.W. Gill, B. Johnson, W. Chen, M.W. Wong, J.L. Andres, C. Gonzalez, M. Head-Gordon, E.S. Replogle, J.A. Pople, Gaussian 03, Revision C. 01, Gaussian Inc., Pittsburgh, PA, 2003.
[23] B. Liu, A.D. McLean, J. Chem. Phys. 59 (1973) 4557.
[24] N. Mukawa, T. Goto, H. Nariai, Y. Aoki, A. Imamura, T. Takeuchi, J. Pharm. Biomed. Anal. 30 (2003) 1943.
[25] J.C. Slater, The Self-consistent Field for Molecules and Solids: Quantum Theory of Molecules and Solids, vol. 4, McGraw-Hill, New York, 1974.
[26] C.J. Cramer, Essentials of Computational Chemistry: Theories and Models, 2nd ed., John Wiley & Sons, Chichester, England, 2004.
[27] F. Jensen, Introduction to Computational Chemistry, 2nd ed., John Wiley & Sons, Inc., Chichester, England, 2007.
[28] K.V. Mikkelsen, H. Ågren, J. Mol. Struct. (Theochem.) 234 (1991) 425.
[29] C.J. Cramer, D.G. Truhlar, Chem. Rev. 99 (1999) 2161.
[30] P.E. Smith, B.M. Pettitt, J. Phys. Chem. 98 (1994) 9700.
[31] B. Roux, T. Simonson, Biophys. Chem. 78 (1999) 1.
[32] M. Cossi, V. Barone, R. Cammi, J. Tomasi, Chem. Phys. Lett. 255 (1996) 327.
[33] J. Tomasi, M. Persico, Chem. Rev. 94 (1994) 2027.
[34] S. Miertus, G. Scrocco, J. Tomasi, Chem. Phys. 55 (1981) 117.
[35] S. Miertus, J. Tomasi, Chem. Phys. 65 (1982) 239.
[36] S.A. Piletsky, K. Karim, E.V. Piletska, C.J. Day, D.W. Freebairn, C. Legge, A.P.F. Turner, Analyst 126 (2001) 1826.
[37] R.J. Umpleby, S.C. Baxter, Y. Chen, R.N. Shah, K.D. Shimizu, Anal. Chem. 73 (2001) 4584.
[38] D.K. Gosser, Cyclic Voltammetry: Simulation and Analysis of Reaction Mechanisms, VSH, New York, 1993.
[39] A.M. Bond, Modern Polarographic Methods in Analytical Chemistry, Dekker (Marcel), New York, 1980.
[40] A.J. Bard, L.R. Faulkner, Electrochemical Methods: Fundamentals and Applications, 2nd ed., John Wiley & Sons, New York, 2000.
[41] Clark's Analysis of Drugs and Poisons, 3rd ed., Pharmaceutical Press, London, UK, 2004.
[42] E.E. Chufán, F.D. Suvire, R.D. Enriz, J.C. Pedregosa, Talanta 49 (1999) 859.
[43] S. Piletsky, A. Turner, Molecular Imprinting of Polymers, Landes Bioscience, Texas, USA, 2006.
[44] European Pharmacopoeia, 4th ed., European Department for the Quality of Medicines, Strasbourg, France, 2002.